STM INVESTIGATION OF PHTHALOCYANINES AS POSSIBLE BUILDING BLOCKS FOR QUANTUM-DOT CELLULAR AUTOMATA

A Thesis

Submitted to the Graduate School

of the University of Notre Dame

in Partial Fulfillment of the Requirements

for the Degree of

Master of Science

by

Adam Christopher Beck, B.S.

_____

S. Alex Kandel, Director

Graduate Program in Chemistry and Biochemistry

Notre Dame, Indiana

November 2005

STM INVESTIGATION OF PHTHALOCYANINES AS POSSIBLE BUILDING BLOCKS FOR QUANTUM-DOT CELLULAR AUTOMATA

Abstract

by

Adam Christopher Beck

Ultra-high-vacuum scanning tunneling microscopy was used to observe copper phthalocyanine molecules deposited on the Au(111) surface. The primary goal of these experiments was to isolate a single copper phthalocyanine so that its electronic properties could be studied closely with the molecule not interacting with any other surface bound molecules.

There where several issues that had to be addressed satisfactorily before the microscope would be ready to scan single molecules. These steps included fabricating a support structure for the instrument, and eliminating or minimizing all sources of external noise. Several samples were used to calibrate the microscope and verify that the instrument could image atomic-scale features.

Dip-casting was used to create Au(111) samples with low coverages of copper phthalocyanines. We optimized the experimental parameters used to acquire images, including bias voltage, tunneling current, and scan speed; this optimization was done to maximize resolution, contrast, and tunneling stability. STM imaging of single copper phthalocyanine molecules was demonstrated.

CONTENTS

FIGURES

CHAPTER 1

INTRODUCTION

1.1 Molecular Electronics

At a point in the near future, electronic devices will reach their minimal functioning size. Material properties that are well understood at the macroscopic scale do not describe systems at the molecular level[1, 2]: insulators do not insulate, conductors do not conduct, and semiconductors exhibit quantum behavior.[3] There is additional difficulty in fabricating electronic devices, as currently used photolithography techniques are becoming exponentially more expensive as the features in electronic devices become smaller.[4] This is where molecular electronics comes in, with the goal of fabricating electrical devices from groups of single molecules.[5, 6] Creating electrical devices from groups of single molecules would utilize the smallest building material known, and would allow for the creation of the smallest possible electronic devices.

The major advantage of molecule-based electronics is the small feature size. Additional benefits arise from the application of organic and inorganic synthetic techniques. Synthetic chemistry has developed tools that allow atomic structures to be created with precisely specified three-dimensional geometries. Synthesis is a laboratory setting inherently produces molecules with identical atomic structures, and

produces them in tremendous (10^23) quantities. This is in contrast to traditional silicon-based electronic devices. Current devices require ultra-high-purity silicon; atomically precise devices would raise standards for purity astronomically. Additionally, tolerances of lithographic processing, which is inherently a macroscopic technique, are not tight enough for very small feature sizes, where the placement of a single atom can have a substantial impact on device characteristics.[5]

There are various benefits to utilizing a molecular electronics system; however, there are certain drawbacks that must be addressed when fabricating such a system. First, there must be a practical, accurate, repeatable, and fast method to manipulate the molecules into desired patterns and keep them in place. Second, there must be an interface in place to the macroscopic world that can read and write data to and from the molecular system.

1.2 Quantum-dot Cellular Automata

While there are several different approaches on how single molecules may be used to create electronic devices,[7-10] the approach focused on in this thesis is that of Quantum-dot Cellular Automata (QCA).[11-15] The building block for QCA is the QCA cell. Figure 1.1(a) and (b) illustrate the four-dot, two-electron QCA cell; an electron can occupy any of the four dots, but electron-electron repulsion creates two low-energy configurations that a two-electron cell may adopt, shown as “0” and “1”. Coulombic interactions between adjacent cells means that the state of one cell will affect the state of all nearby cells. For example, for two side-by-side cells, if one is in configuration “1”, the other will be affected by this and change its configuration to

"1" as well. Thus, multiple cell-cell interactions mean that chains of cells propagate information, and complex networks perform computations such as logic gates (AND/OR) and addition.[16, 17] The two-dot, one-electron cell (shown in Figure 1.1(c) and (d)) behave in much the same way as the four-dot cell.

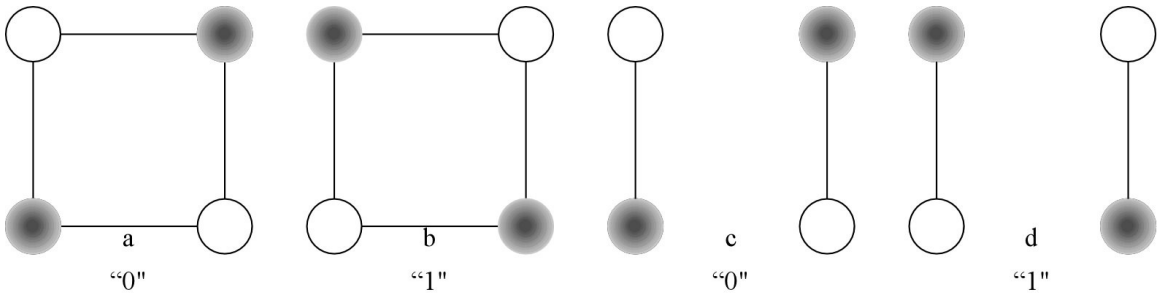

Figure 1.1 QCA molecules consist of either four oxidation sites like in (a) and (b), or two oxidation sites like those shown in (c) and (d). In both cases the oxidations sites will be are tethered together using a chain that electrons are capable of tunneling through. The number in the figure are an arbitrary labeling of charge positions in the molecule.

A molecular QCA cell involves multiple (two or four) oxidation sites; these sites are where excess electrons will be located. These oxidation sites will consist of metal atoms that should be controllably reduced or oxidized.[18, 19] The metal atoms will exchange electrons through the tethers connecting each metal atom. The charge density should be analogous to the diagrams in Figure 1.1 in order for a molecule to function as a QCA cell. The overall charge on the molecule may be positive or negative balanced with a counterion, or the overall charge of the molecule may be neutral.

Laying out a network of QCA cells is most easily accomplished on a surface. Additionally, placing QCA cells on a surface opens up several ways of probing cell properties. The surface should have several important characteristics. The molecules

must be bound tightly enough so that they do not move around. The surface should be chemically inert so that it will not degrade over time. The chemical structure and the electronic properties of the molecule should not be altered by the surface. Finally, the surface structure should be uniform and well understood.

For a molecular QCA device on a surface, the molecules can be placed on the surface in two different geometries, as depicted in Figure 1.2. The molecules can be placed either parallel or perpendicular to the surface, and the orientation of the molecule will affect its interaction with the surface. A molecule lying parallel to the surface maximizes this effect, as all of its oxidation sites interact with the surface. When standing perpendicular to the surface, a molecule's interaction with the surface is lessened, but the interaction is now asymmetric.

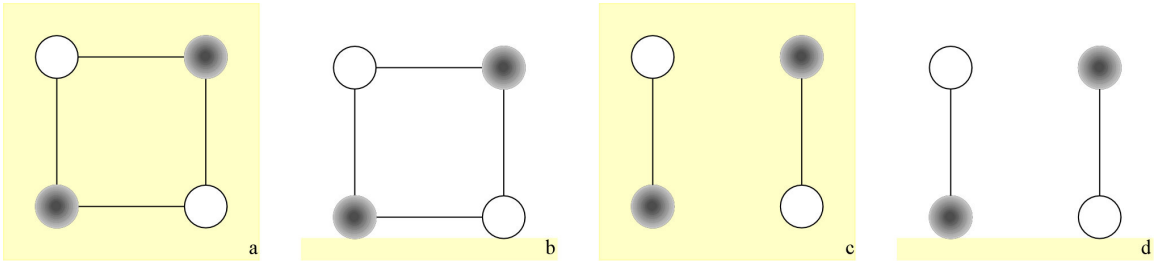

Figure 1.2 Figures (a) and (b) demonstrate two possibilities of how a four-oxidation site QCA molecule could sit on a surface. Figures (c) and (d) demonstrate two possibilities of how a two-oxidation site QCA molecule could sit on a surface.

For either adsorption geometry, there are potential problems that may arise. There are different possible ways to alleviate the problems associated with molecules interacting with the substrate. Three possible ways are (a) using an insulating layer to separate the molecules from the substrate, (b) attaching insulating legs to the molecule to separate it from the substrate, or (c) using an insulating substrate. Our experiments focus on studying the properties of single, surface-bound molecules.

This is important because the behavior of a molecular QCA cell is dependent on its interactions with the surface.

1.3 Scanning Tunneling Microscopy

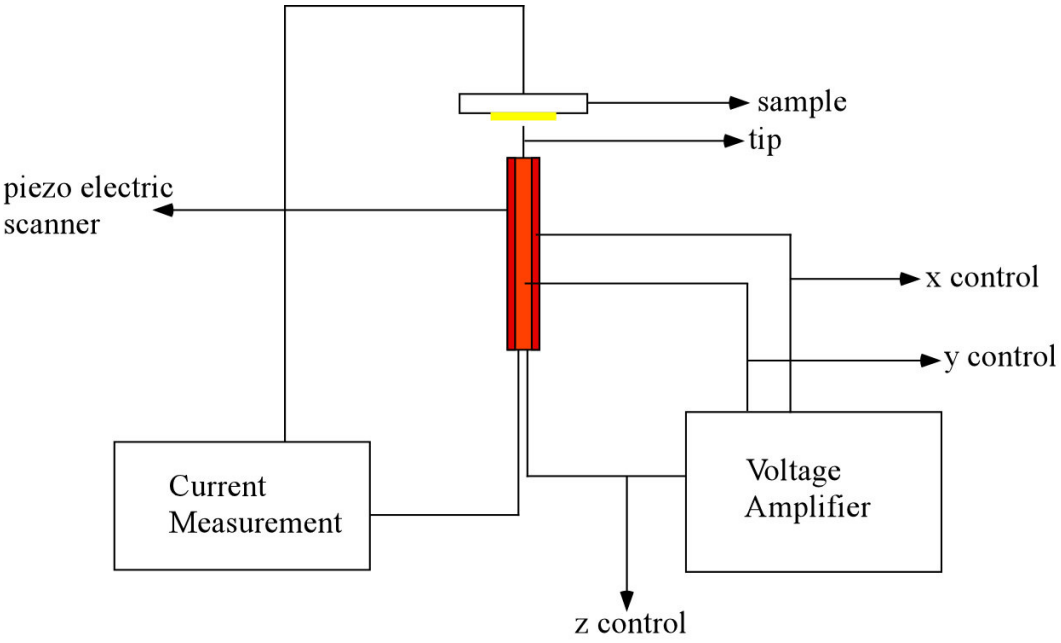

Figure 1.3 Schematic of STM layout.

The technique used to study potential QCA molecules was scanning tunneling microscopy, or STM. Figure 1.3 is a schematic drawing of an STM system. STM has two major methods of use: measuring molecular topography and molecular spectroscopy. These two methods are related because of the basis for STM, which entails electrons tunneling between a tip and a sample. A conductive tip is brought within approximately 1-10 Angstroms of the surface and once within range, a negative or positive bias is placed across the conductive tip.

Topography involves maintaining a constant current and observing how the tip/sample distance is affected. There are two major aspects of a scan that can affect

the current, which are the bias voltage and the tip/sample distance. These two aspects are related themselves in addition to their affect on the current. As the bias voltage is raised, the number of electrons that can tunnel between the tip and sample increases, which correspondingly increases the probability of an electron tunneling between the tip and sample. The current is exponentially related to the tip/sample distance. As this distance becomes smaller, electrons have a greater probability of tunneling between the sample and the tip. During a topography scan the current is held constant and the z position of the tip is read. When the data for this thesis was collected there was a negative bias placed on the tip.

Spectroscopy involves maintaining a constant tip/sample distance and observing how the current is affected by a ramping of the bias voltage. The tip can be placed directly over a molecule on the surface so as to allow the study of electronic properties. The electronic structure of an entire molecule can be probed by placing the tip over different parts of the molecule. The electronic structure of the molecule can affect how the current is altered as the bias voltage is changed.

The STM method used in these experiments was molecular topography. The tip will respond to changes in height on the surface by adjusting its distance from the surface so as to compensate for height changes and maintain a constant current. The current dependence on tip/sample distance allows the tip to respond to a bump or molecule on the surface. The tip will be retracted enough to keep the current at a constant value.

The most important part is the piezo-electric scanner. The piezo-electric scanner refers to a ceramic material that responds with tiny movements when voltages

are applied to it. The responsive movements are only angstroms in magnitude, which is ideal for scanning molecular size images. A tube piezo has five electrodes attached to it, each controlling a different aspect of the piezo-electric device movement. The movements of the piezo are so small that another device is needed to move the tip toward the surface. The movement of the tip toward the surface is done in three steps: the first is a camera used to watch the tip moved by a hand held device to move the tip tens to hundreds of microns away from the surface. The second is a microslider used to move the tip a few hundred nanometers from the surface. Third, the piezoelectric scanner intervenes and moves the tip 1-10 Angstroms away from the surface.

1.4 References

1. Packan, P.A., *Perspectives: Device physics - Pushing the limits.* Science, 1999. **285**(5436): p. 2079-+.

2. Tour, J.M., *Molecular electronics. Synthesis and testing of components.* Accounts of Chemical Research, 2000. **33**(11): p. 791-804.

3. Snider, G.L., A.O. Orlov, I. Amlani, X. Zuo, G.H. Bernstein, C.S. Lent, J.L. Merz, and W. Porod, *Quantum-dot cellular automata: Review and recent experiments (invited).* Journal of Applied Physics, 1999. **85**(8): p. 4283-4285.

4. Service, R.F., *Can chip devices keep shrinking?* Science, 1996. **274**(5294): p. 1834-1836.

5. Carroll, R.L. and C.B. Gorman, *The genesis of molecular electronics.* Angewandte Chemie-International Edition, 2002. **41**(23): p. 4379-4400.

6. Mantooth, B.A. and P.S. Weiss, *Fabrication, assembly, and characterization of molecular electronic components.* Proceedings of the Ieee, 2003. **91**(11): p. 1785-1802.

7. Crone, B., A. Dodabalapur, Y.Y. Lin, R.W. Filas, Z. Bao, A. LaDuca, R. Sarpeshkar, H.E. Katz, and W. Li, *Large-scale complementary integrated circuits based on organic transistors.* Nature, 2000. **403**(6769): p. 521-523.

8. James, D.K. and J.M. Tour, *Electrical measurements in molecular electronics.* Chemistry of Materials, 2004. **16**(23): p. 4423-4435.

9. Watson, M.D., F. Jackel, N. Severin, J.P. Rabe, and K. Mullen, *A hexa-peri-hexabenzocoronene cyclophane: An addition to the toolbox for molecular electronics.* Journal of the American Chemical Society, 2004. **126**(5): p. 1402-1407.

10. Sanders, G.D., K.W. Kim, and W.C. Holton, *Optically driven quantum-dot quantum computer.* Physical Review A, 1999. **60**(5): p. 4146-4149.

11. Lent, C.S., P.D. Tougaw, and W. Porod, *Bistable Saturation in Coupled Quantum Dots for Quantum Cellular Automata.* Applied Physics Letters, 1993. **62**(7): p. 714-716.

12. Lent, C.S., B. Isaksen, and M. Lieberman, *Molecular quantum-dot cellular automata.* Journal of the American Chemical Society, 2003. **125**(4): p. 1056-1063.

13. Lent, C.S. and P.D. Tougaw, *Lines of Interacting Quantum-Dot Cells - a Binary Wire.* Journal of Applied Physics, 1993. **74**(10): p. 6227-6233.

14. Manimaran, M., G.L. Snider, C.S. Lent, V. Sarveswaran, M. Lieberman, Z.H. Li, and T.P. Fehlner, *Scanning tunneling microscopy and spectroscopy investigations of QCA molecules.* Ultramicroscopy, 2003. **97**(1-4): p. 55-63.

15. Orlov, A.O., I. Amlani, R.K. Kummamuru, R. Ramasubramaniam, G. Toth, C.S. Lent, G.H. Bernstein, and G.L. Snider, *Experimental demonstration of clocked single-electron switching in quantum-dot cellular automata.* Applied Physics Letters, 2000. **77**(2): p. 295-297.

16. Tougaw, P.D. and C.S. Lent, *Logical Devices Implemented Using Quantum Cellular-Automata.* Journal of Applied Physics, 1994. **75**(3): p. 1818-1825.

17. Lent, C.S. and P.D. Tougaw, *Bistable Saturation Due to Single-Electron Charging in Rings of Tunnel-Junctions.* Journal of Applied Physics, 1994. **75**(8): p. 4077-4080.

18. Orlov, A.O., R. Kummamuru, R. Ramasubramaniam, C.S. Lent, G.H. Bernstein, and G.L. Snider, *Clocked quantum-dot cellular automata shift register.* Surface Science, 2003. **532**: p. 1193-1198.

19. Toth, G. and C.S. Lent, *Quasiadiabatic switching for metal-island quantum-dot cellular automata.* Journal of Applied Physics, 1999. **85**(5): p. 2977-2984.

CHAPTER 2

BACKGROUND

2.1 Phthalocyanines

The general structure for phthalocyanines can be seen in Figure 2.1. The four symmetrical pi-systems are located through the nitrogen and aromatic carbon rings in each corner. Various functional groups may be attached to the outer carbon atoms. Physical and electronic structure of surface-bound phthalocyanines have previously been studied extensively using STM.[1-10] These studies included use of different surfaces,[11] different metal centers for the phthalocyanines, and a wide range of functional groups connected to the phthalocyanines.[12]

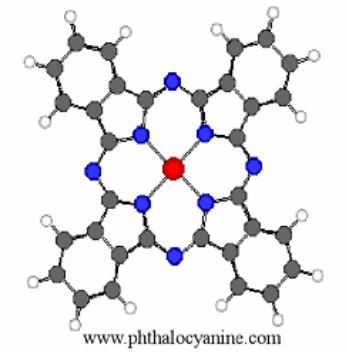

Figure 2.1 This is a general layout of a phthalocyanine with the blue dots indicating a nitrogen atom, the gray dots indicating a carbon atom, and the middle red dot signifying a metal atom. www.phthalocyanine.com

2.2 Previous Studies

There exist only a few studies directed at single, stationary phthalocyanines that are not interacting with other phthalocyanines or other surface bound molecules.[13, 14] When phthalocyanines are packed into full monolayers, adjacent molecules interact with each other through van der Waals forces. The temperature at which these molecules are studied may determine how well the internal structure of the molecule can be observed by STM. At lower temperatures, the amount of thermal energy in the phthalocyanine/substrate system may be lowered enough so that the phthalocyanines move much slower on the surface, or not at all.

2.2.1 Sub-Molecular Resolution

Previous studies of phthalocyanines have shown sub-molecular resolution[2], as seen in Figure 2.2.[15, 16]

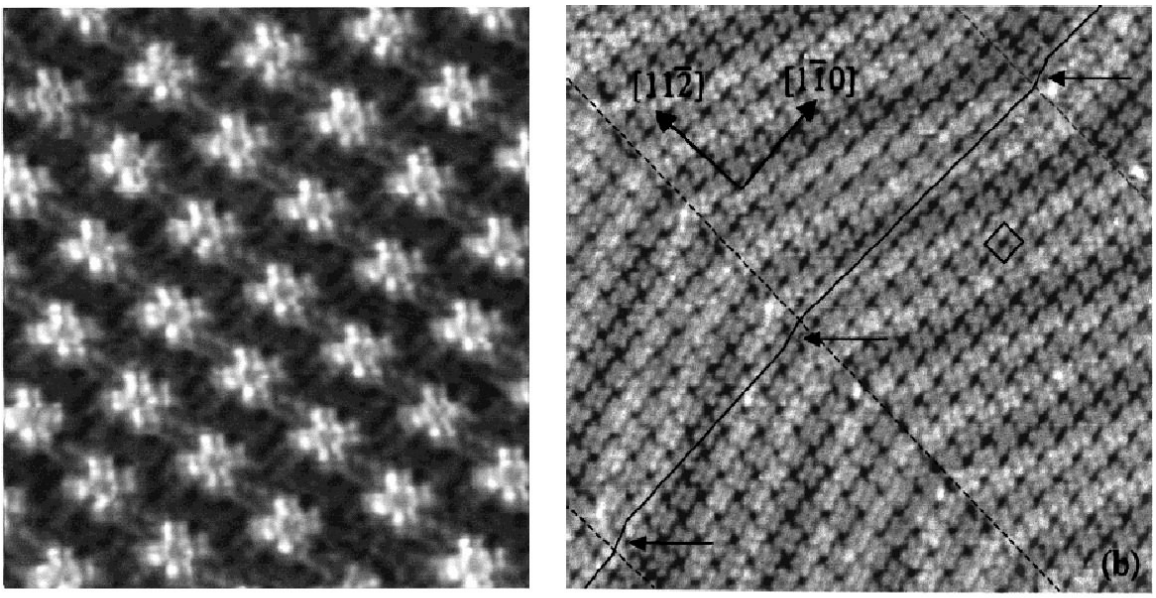

a b

Figure 2.2 (a) Xiaohui Qiu, Chen Wang, Shuxia Yin, Qingdao Zeng, Bo Xu, and Chunli Bai, *J. Phys. Chem. B*, Vol. 104, No. 15, *2000* this image depicts sub-molecular resolution of a phthalocyanine placed on a HOPG surface with tunneling conditions of 398 pA and -648 mV.
(b) I. Chizhov, G. Scoles, and A. Kahn, *Langmuir*, **2000**, *16*, 4358-4361 This image depicts how phthalocyanines follow the underlying structure of the surface. Here the phthalocyanines follow the herring-bone structure along the gold surface.

The sub-molecular images in Figure 2.2 provide the detail that can be observed using STM to study phthalocyanines. In both images (a) and (b) of Figure 2.2 a full monolayer of phthalocyanines is shown. There is minimal motion in both images, as the phthalocyanines are locked into place due to the van der Waals forces between adjacent surface bound molecules. Figure 2.2(a) shows the precise detail that can be attained using STM, while Figure 2.2(b) depicts how phthalocyanines follow substrate patterning. In Figure 2.2(a), the distinct pi-systems can be seen as the four bulges around a central hole in each four-leaf clover structure. The octane arms attached to the pi-systems can be seen as the light gray structures protruding from each of the four bulges located on the main structure. Figure 2.2(b) depicts the

phthalocyanines following the herringbone reconstruction on the gold surface. The diagonal black line drawn on the surface follow the center of the phthalocyanines and shows that with each kink in the herringbone reconstruction, the phthalocyanines on the surface follow the gold reconstruction.

2.2.2 Phthalocyanines and Other Molecules

Phthalocyanines can also be adsorbed along with other molecules.[1, 17] Figure 2.3[18] shows phthalocyanines adsorbed with octodecanethiol.

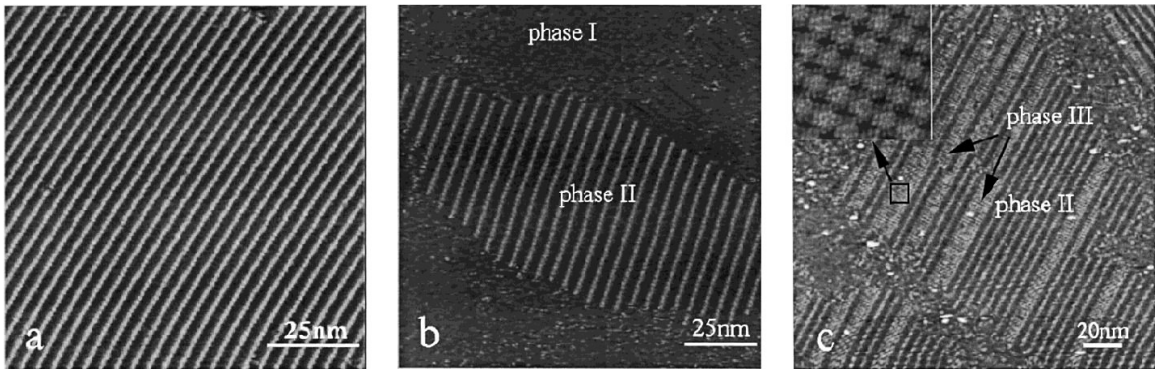

Figure 2.3 S.B. Lei, C. Wang, S. X. Yin, and C.L. Bai, *J. Phys. Chem. B*, Vol. 105, No. 49, *2001* Images (a), (b), and (c) show different ratios of octodecanethiol to phthalocyanine. (a) shows what occurs when the ratio is 3:1 (b) shows what occurs when the ratio is greater than 3:1 (c) shows what occurs when the ratio is less than 3:1. The box in the upper left hand corner is a zoom-in on an area that contains only phthalocyanines.

Figure 2.3 shows that using other molecules reduces the motion of the phthalocyanines on the surface. The interactions between the thiols and the phthalocyanines are van der Waals in nature, just as those between adjacent phthalocyanines. The amount of the three particular phases is tied to the ratio of phthalocyanine to octodecanethiol. In Figure 2.3(a), the ratio is 1:3, phthalocyanine to octodecanethiol, creating the lined structures. The black lines are the octodecanethiols laying on theirs sides and the white lines are the phthalocyanines.

Figure 2.3(b) has a ratio greater than 1:3, and Figure 2.3(c) has a ratio less than 1:3. The three phases present in Figure 2.3 are: (I) representing the 1:3 ratio in which the octodecanethiols and phthalocyanines create the line structures, (II) signifies phases that consist of only octodecanethiol, and (III) represents areas consisting only of phthalocyanines. Figure 2.3(c) contains a magnification of an area entirely covered with phthalocyanines. The magnified area indicates molecular resolution of the phthalocyanines, parts of the molecule can be seen. However, greater detail is needed to better understand the physical and electronic properties to the phthalocyanines. The phthalocyanines are held in place by the octodecanethiols and the interactions between the two surface molecules are sufficient to reduce the motion of the phthalocyanines to allow for high resolution images. Figure 2.4[18] shows a magnification of a group of phthalocyanines that are trapped by the octodecanethiol.

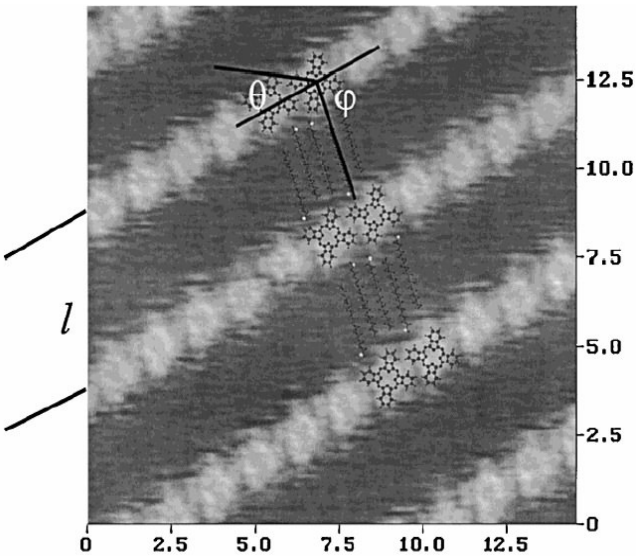

Figure 2.4 S.B. Lei, C. Wang, S. X. Yin, and C.L. Bai, *J. Phys. Chem. B*, Vol. 105, No. 49, *2001* This image is a blow up of the line structures that are seen in Figure 14. The fine structure of both the phthalocyanines and thiols are drawn out in the picture. The thiols are laying on their sides, while the phthalocyanines are laying flat on the surface.

2.2.3 Coverage Less Than One Monolayer

Phthalocyanines have been studied with a coverage less than a single monolayer and not in conjunction with another molecule. The images below contain less than a full monolayer of phthalocyanines.[11, 19]

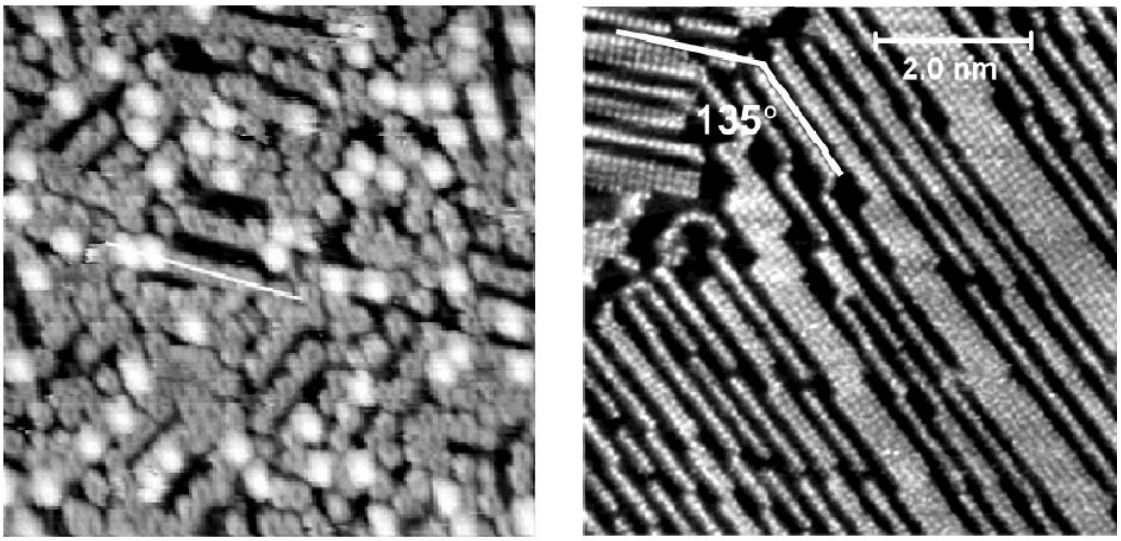

a b

Figure 2.5 (a) K. Walzer, M. Hietschold, *Surface Science*, 471 (2001) 1-10 This image shows a less than full monolayer coverage of a phthalocyanine on a graphite surface. Each doughnut structure represents a single phthalocyanine.
(b) Dan E. Barlow, L. Scudiero, and K.W. Hipps, *Langmuir*, Vol. 20, No. 11, *2004* This image represents a less than full monolayer coverage of a phthalocyanine on an Au(111) surface. Each white dot is a single phthalocyanine. Because the coverage is high enough, phthalocyanines group together stabilizing each other.

Figure 2.5(a) depicts a phthalocyanine with a tin atom at the center adsorbed on graphite, at a temperature of 35 K. The lower temperature has frozen the phthalocyanines in the same spot on the surface reflecting no translational motion. However rotational motion still remains a hindrance to sub-molecular resolution. An explanation for the doughnut shape structure in Figure 2.5(a) are that the tin atoms at the center of the phthalocyanines are imaged as dark spots. The bright spots located throughout the image are phthalocyanines stacked on top of each other. Figure 2.5(b)

was scanned at room temperature and the surface coverage was greater than that of Figure 2.5(a). Both Figure 2.5(a) and (b) have single molecule resolution, however neither surface coverage allows for an isolated phthalocyanine to be studied with no interactions with other surface bound molecules.

In the images shown above, we have seen that STM is a powerful tool for studying phthalocyanines. Under proper tunneling conditions and with a sharp tip, sub-molecular resolution is attainable. In the studies above the phthalocyanine molecules are held in place by different methods, either using full monolayers or partial monolayers with lowered temperatures. There is one similarity, the phthalocyanines in all the images are interacting with other surface-bound molecules, whether they be other different molecules or other phthalocyanines.

2.3 Phthalocyanine Movement

The conditions of the images shown above were in place to limit the movement of the phthalocyanines. Phthalocyanine movement can be in one of two different modes. The first is translational motion, which is the molecule moving laterally across the surface. The second mode is rotational motion; in this case part of the phthalocyanine is bound to the surface and becomes an axis of rotation for the entire molecule. There are different system modifications that may be utilized to reduce translational motion. One such modification is full monolayer coverage keeping the phthalocyanines still due to the interactions between the molecules.[20] A second modification is altering the chains attached to the outer carbons in the phthalocyanine so the interactions between

the surface and the molecule is stronger, keeping the molecule in place.[21] Of these two motions, rotational motion are more difficult to stop.

There are numerous examples of phthalocyanine studies on surfaces that contain other molecules. The previous figures show phthalocyanines interacting with other types of molecules as well as interacting with each other. These figures also show that sub-molecular resolution is possible when studying phthalocyanines with STM.

2.4 References

1. Hipps, K.W., X. Lu, X.D. Wang, and U. Mazur, *Metal d-orbital occupation-dependent images in the scanning: Tunneling microscopy of metal phthalocyanines.* Journal of Physical Chemistry, 1996. **100**(27): p. 11207-11210.

2. Ludwig, C., R. Strohmaier, J. Petersen, B. Gompf, and W. Eisenmenger, *Epitaxy and Scanning-Tunneling-Microscopy Image-Contrast of Copper Phthalocyanine on Graphite and Mos2.* Journal of Vacuum Science & Technology B, 1994. **12**(3): p. 1963-1966.

3. Garnier, F., *Thin-film transistors based on organic conjugated semiconductors.* Chemical Physics, 1998. **227**(1-2): p. 253-262.

4. Bao, Z.A., A.J. Lovinger, and J. Brown, *New air-stable n-channel organic thin film transistors.* Journal of the American Chemical Society, 1998. **120**(1): p. 207-208.

5. Madru, R., G. Guillaud, M. Alsadoun, M. Maitrot, J.J. Andre, J. Simon, and R. Even, *A Well-Behaved Field-Effect Transistor Based on an Intrinsic Molecular Semiconductor.* Chemical Physics Letters, 1988. **145**(4): p. 343-346.

6. Maitrot, M., G. Guillaud, B. Boudjema, J.J. Andre, H. Strzelecka, J. Simon, and R. Even, *Lutetium Bisphthalocyanine - the 1st Molecular Semiconductor - Conduction Properties of Thin-Films of P-Doped and N-Doped Materials.* Chemical Physics Letters, 1987. **133**(1): p. 59-62.

7. Collins, R.A. and K.A. Mohammed, *Gas Sensitivity of Some Metal Phthalocyanines.* Journal of Physics D-Applied Physics, 1988. **21**(1): p. 154-161.

8. Hiesgen, R., M. Rabisch, H. Bottcher, and D. Meissner, *STM investigation of the growth structure of Cu-phthalocyanine films with submolecular resolution.* Solar Energy Materials and Solar Cells, 2000. **61**(1): p. 73-85.

9. Bohringer, M., R. Berndt, and W.D. Schneider, *Transition from three-dimensional to two-dimensional faceting of Ag(110) induced by Cu-phthalocyanine.* Physical Review B, 1997. **55**(3): p. 1384-1387.

10. Kanai, M., T. Kawai, K. Motai, X.D. Wang, T. Hashizume, and T. Sakura, *Scanning-Tunneling-Microscopy Observation of Copper-Phthalocyanine Molecules on Si(100) and Si(111) Surfaces.* Surface Science, 1995. **329**(3): p. L619-L623.

11. Walzer, K. and M. Hietschold, *STM and STS investigation of ultrathin tin phthalocyanine layers adsorbed on HOPG(0001) and Au(111).* Surface Science, 2001. **471**(1-3): p. 1-10.

12. Inabe, T. and H. Tajima, *Phthalocyanines - Versatile components of molecular conductors.* Chemical Reviews, 2004. **104**(11): p. 5503-5533.

13. Lippel, P.H., R.J. Wilson, M.D. Miller, C. Woll, and S. Chiang, *High-Resolution Imaging of Copper-Phthalocyanine by Scanning-Tunneling Microscopy.* Physical Review Letters, 1989. **62**(2): p. 171-174.

14. Gimzewski, J.K., E. Stoll, and R.R. Schlittler, *Scanning Tunneling Microscopy of Individual Molecules of Copper Phthalocyanine Adsorbed on Polycrystalline Silver Surfaces.* Surface Science, 1987. **181**(1-2): p. 267-277.

15. Qiu, X.H., C. Wang, S.X. Yin, Q.D. Zeng, B. Xu, and C.L. Bai, *Self-assembly and immobilization of metallophthalocyanines by alkyl substituents observed with scanning tunneling microscopy.* Journal of Physical Chemistry B, 2000. **104**(15): p. 3570-3574.

16. Chizhov, I., G. Scoles, and A. Kahn, *The influence of steps on the orientation of copper phthalocyanine monolayers on Au(111).* Langmuir, 2000. **16**(9): p. 4358-4361.

17. Stohr, M., T. Wagner, M. Gabriel, B. Weyers, and R. Moller, *Binary molecular layers of C-60 and copper phthalocyanine on Au(111): Self-organized nanostructuring.* Advanced Functional Materials, 2001. **11**(3): p. 175-178.

18. Lei, S.B., C. Wang, S.X. Yin, and C.L. Bai, *Single molecular arrays of phthalocyanine assembled with nanometer sized alkane templates.* Journal of Physical Chemistry B, 2001. **105**(49): p. 12272-12277.

19. Barlow, D.E., L. Scudiero, and K.W. Hipps, *Scanning tunneling microscopy study of the structure and orbital-mediated tunneling spectra of cobalt(II) phthalocyanine and cobalt(II) tetraphenylporphyrin on Au(111): Mixed composition films.* Langmuir, 2004. **20**(11): p. 4413-4421.

20. Grand, J.Y., T. Kunstmann, D. Hoffmann, A. Haas, M. Dietsche, J. Seifritz, and R. Moller, *Epitaxial growth of copper phthalocyanine monolayers on Ag(111).* Surface Science, 1996. **366**(3): p. 403-414.

21. Jung, T.A., R.R. Schlittler, J.K. Gimzewski, H. Tang, and C. Joachim, *Controlled room-temperature positioning of individual molecules: Molecular flexure and motion.* Science, 1996. **271**(5246): p. 181-184.

CHAPTER 3

EXPERIMENTAL

3.1 Instrumentation

The instrumentation used for the experiments described in this thesis was a low temperature scanning tunneling microscope (LT-STM), depicted in Figure 3.1, fabricated by Omicron Nanotechnology. Rather than purchasing a complete STM system from Omicron, we purchased their low-temperature STM and vacuum chamber, and assembled these with our own pumps, gauges, and flanges, and built our own instrument support structure. This resulted in a substantial savings in cost.

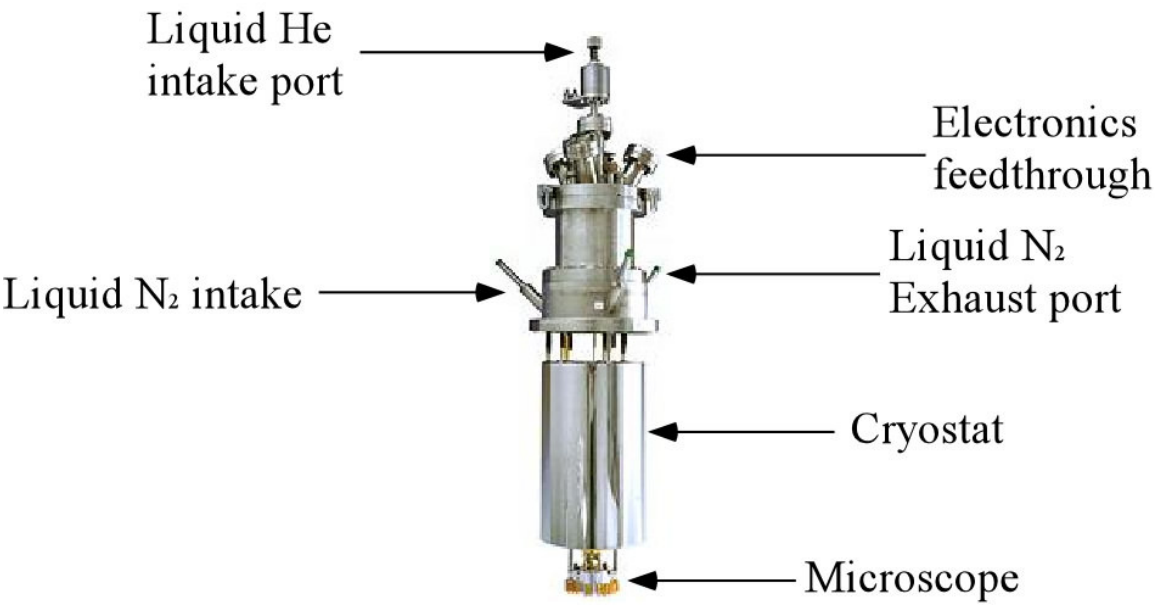

Figure 3.1 The figure above was taken from the Omicron Nanotechnology website. www.omicron.de/products/spm/low_temperature_instruments/lt_stm/index.html

The table on which the LT-STM is situated had several requirements that had to be taken into account. The system had to be sturdy enough to support a large amount of weight, rigid enough so not to introduce vibrational resonances into the system, had to provide a suitable system bake-out, and had to supply vibration isolation. In order to adhere to the requirements set, the table was built from square, hollow steel beams which were welded together to create a solid frame weighing about 100 pounds.

The microscope is housed at the bottom of Figure 3.1. The hollow stainless steel cylinder hanging off the flange is the cryostat; this can be filled with liquid nitrogen to cool the microscope to 78 K. There is an inner cryostat chamber that can be filled with liquid helium, lowering the microscope temperature to beyond 78 K. The table had to be capable of supporting such a system, as well as take into account the height of the chamber. With the liquid helium line attached to the top of the LT-STM, the entire apparatus stands at approximately 10 feet in height.

One of the components of the apparatus that had to be taken into account when building the table was the large ion pump attached to the bottom of the chamber. The connection between the pump and the chamber needed to be air tight; the smallest leak would not allow the system to be pumped down to the desired ultra high vacuum conditions. The gasket connection between the pump and the chamber is not designed to support the weight of the ion pump. The ion pump needed to be supported in some other way than just the pump chamber connection. The was accomplished using four aluminum bars attached to the chamber. These four aluminum bars were then bolted to Unistrut™ bars that had been fixed to the table.

Once the aluminum bars were bolted to the Unistrut™, the pump was able to hang freely from the table, keeping the strain on the pump/chamber connection to a minimum.

An oven was created by using perforated aluminum angle stock to create a box frame around the chamber with heaters placed inside the frame. Initially, pieces of sheet metal were used, bolted around the frame, but these were difficult to work with. Therefore, we decided on welders blankets to cover the frame. The heaters used consisted of fans with variable current running through them, the temperature needed to be controlled due to heating restrictions of piezo-electric scanner. The temperature of the instrument was monitored using thermocouples attached to the vacuum chamber.

The entire apparatus is held using four Newport Stabilizer™ High Performance Laminar Flow Isolators, I-2000 series. These pneumatic isolators have a line of nitrogen gas constantly fed to them, which allows them to vibrationally isolate the table from the ground. The pneumatic isolators do not negate all of the vibrations in the laboratory; however they successfully minimized many of the problem frequencies. The vibrations of the table were measured before every approach using a seismometer, and the isolators were adjusted as necessary to minimize the vibrations detected by the seismometer. Figure 3.2 shows the final setup of the chamber on the table.

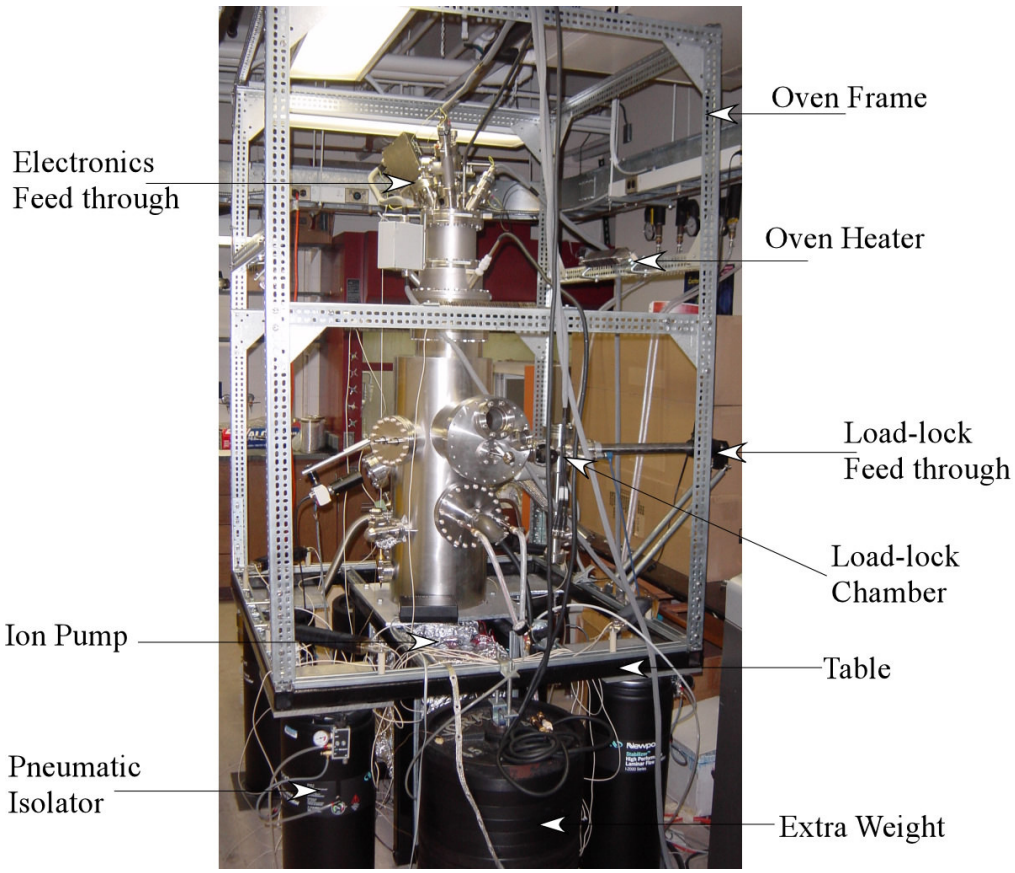

Figure 3.2 Microscope and table after all accessories have been assembled and attached to the table

3.2 Tip

The component that makes STM possible is the tip, which can be made from any conductive material. A platinum/iridium alloy tip was used for these experiments. The tip is the instrument: all the information that is recorded from the instrument comes from the interactions between the tip and the sample. An ideal tip would have a single atom at its very end.

Examples of what could go wrong with the tip include: a double tip, a blunt tip, and tip instability. A double tip is when there are two atoms at the end of the tip that are equal distances away from the surface, yet far enough away from each other

to not blur the image. When this occurs, features on the surface will be scanned twice, showing two overlapping images in the scan window. These twin features are caused by a tip construction shown in Figure 3.3(a). A blunt tip occurs when a cluster of several atoms are the closest to the surface, as shown in Figure 3.3(b). In this case the number of atoms will blur out the image because electrons are able to tunnel through several atoms equally. Lastly, tip instability can be caused by electrons flowing in or out of the tip. As the electrons flow through the tip, high electric fields are created. These electric fields can cause atoms to rearrange themselves at the end of the tip mid-scan. When atoms move around on the tip during a scan, the tunneling atom continuously moves, and this can blur the image, as shown in Figure 3.3(c) and (d). As electrons move through the tip, atoms can jump to different positions at the end of the tip, as shown with the blue dot.

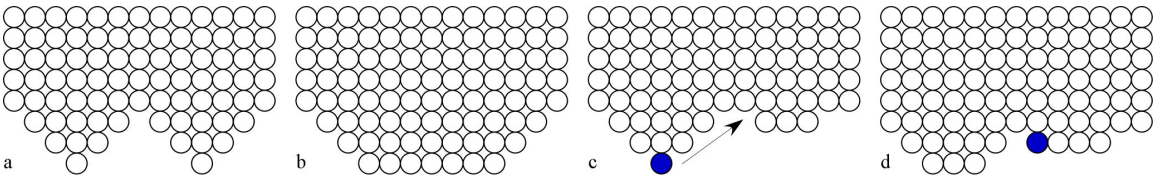

Figure 3.3 Each image displays a different tip problem that may arise (a) double tip, (b) blunt tip, (c) and (d) present instability that may be present when atoms rearrange themselves at the end of the tip

Correcting tip problems can be done several different ways, depending on the conditions. One example of fixing the tip is to clip its end. Clipping is the most straightforward method, with the tip being taken out of vacuum and cut with a clean pair of clippers. The end of the tip is the section of the tip that is angstroms away from the surface. By clipping the end of the tip, any nonconductive material that has gathered on the end of the tip will be removed. The second, but less likely possibility,

is that once the end is cut, the tip will become much sharper. If the tip is cut at a slight angle, the desired result that may be obtained is that the end of the tip will then be only a single atom, which will provide much higher-resolution images. Clipping the tip does not always alleviate tip problems; it may actually ruin the tip.

Another method for improving the tip is a controlled touching of a conductive substrate with the tip. When scanning, it is not necessary for the atoms that mediate electron tunneling to be comprised of the same material. When a tip touches a substrate, the end will bury itself slightly into the substrate. Once buried, several atoms may cling to the end of the tip or several moving atoms that were the cause of an unstable tip may be deposited on the surface. It does not matter if some conductive material clings to the tip, because if the tip is stable, electrons can still flow through the conductive material. If unstable atoms are deposited on the surface, the tip may become more stable allowing for higher resolution images.

Stabilizing the tip can also be done by placing a large bias on the tip. This allows a great number of electrons to tunnel into the surface. This large bias can cause unstable atoms to release from the end of the tip, or conductive atoms from the substrate to be picked up. With the exchange of atoms, it is possible for a single atom to be placed at the end of the tip.

3.3 Sample Preparation

Sample preparation depended on what type of substrate was being used. Graphite samples were prepared by cleaving the graphite surface. Graphite consists of sheets of 6-membered carbon rings layered on top of each other. If a graphite surface is

uneven or contaminated, or has molecules bound to it, the graphite is cleaved. Cleaving involves the surface being placed on a piece of Scotch tape, and ripped away from the tape. Ripping away the tape tears away several layers of carbon rings, revealing a clean, organized surface.

When preparing a sample to be studied with a gold on mica substrate, the first step to preparation is making sure the substrate is cleaned. Cleaning gold involves exposing a hydrogen flame over the substrate for approximately five minutes, a process called annealing. To avoid the gold sample from becoming polycrystalline, one particular area of the sample cannot be exposed to the hydrogen flame for a prolonged period of time. There are two things that are happening to the surface as it is exposed to the flame: the surface is being cleaned, and the heat from the flame allows the gold to reorganize into a hexagonally packed structure.

3.4 Noise

Once scanning began, there was a great deal of noise found in the system. There were several different types of noise, both periodic and aperiodic, that may have been the cause of the problems. The possible types of noise were: acoustic noise, vibrational noise, tip instability, and electrical noise.

Acoustic vibrations could affect the system to which the microscope is attached. If the vacuum chamber begins vibrating from acoustic oscillations, the microscope will display these effects. A simple diagnostic test that can be conducted to determine if acoustic noise is a problem, involves simply dropping a book on a table, creating a sudden sound, and watching the oscilloscope to see if there are any

sudden changes in the current readout. In this case the oscilloscope showed no signs of the current being affected by the loud noise and acoustic noise was found not to be a problem.

When acoustic noise was found not to be a problem, we next sought to isolate vibrational noise. Vibrational noise was the hardest to alleviate because of the numerous places it may arise. This included natural vibrational frequencies within the laboratory as well as the building. One of the advantages of having such a heavy ion pump attached to the bottom of the chamber was that the center of gravity was lowered. An additional advantage was that by adding such a large amount of weight, the resonance frequency of the entire apparatus was lowered. As we progressed, however, the vibrational frequencies were still causing problems. Therefore, we then added 45 pound weights. These additional weights were set on a rod that had been attached to both sides of the table. After adding 1090 pounds, the vibrational frequencies lessened; however, the pneumatic isolators still needed to be optimized manually prior to any approach with the tip.

Once the vibrational frequencies were minimized, the next step became eliminating electronic noise. There was a recurring problem encountered at 60 Hz, which resulted from electrical coupling from the power line to the current-detection electronics, most likely as a result of grounding problems. The first step taken was to ensure everything attached to the microscope was properly grounded; this included all nonelectrical parts connected to the microscope, such as the table. After everything attached to the microscope was properly grounded using a heavy braided tinned-copper wire connected to a communal copper grounding strip in the lab, the 60 Hz

trace seen on the oscilloscope was reduced considerably. The 60 Hz was reduced enough to scan but was never completely eliminated.

After the noise frequencies had been minimized, the last aspect of the LT-STM requiring adjustment was ensuring the LT-STM stood straight inside the vacuum chamber. This had to be done because of the tight tolerances between the microscope stage, which hangs on isolating springs inside the vacuum chamber, and the cryostat walls. If the LT-STM is leaning at a slight angle in any direction then the microscope stage and the cryostat would be touching, and the vibrational isolation that the microscope had from the vacuum chamber would be lost.

3.5 Diagnostic Samples

Once the vacuum chamber was securely fastened to the table and the LT-STM inserted into the vacuum chamber, and the problems discussed above were satisfactorily resolved, three diagnostic samples were scanned to ensure the microscope was in proper working condition: gold on silicon, highly organized pyrolitic graphite (HOPG), and gold on mica. Gold on silicon is a polycrystalline sample with large features. Graphite was scanned next because it has small scale features that tested how the ability of the microscope to achieve atomically resolved images. Finally, gold on mica was scanned because it has small scale features like graphite, but it proved much harder to obtain atomic resolution. Once atomic resolution was seen with gold on mica, the microscope was working properly in all aspects and ready for more complicated systems.

3.5.1 Au on Si

Due to the large surface features, gold on silicon was used to resolve many of the problems. These large features were looked at to determine if the scope could display stable tunneling, repeatably image the same surface area, zoom in on interesting surface features. These tests could have been performed with a Au(111) surface, but the gold on silicon sample was readily available and there was very little preparation time needed to have the sample ready for tunneling. Figure 3.4 depicts several images of gold on silicon, showing the polycrystalline structure.

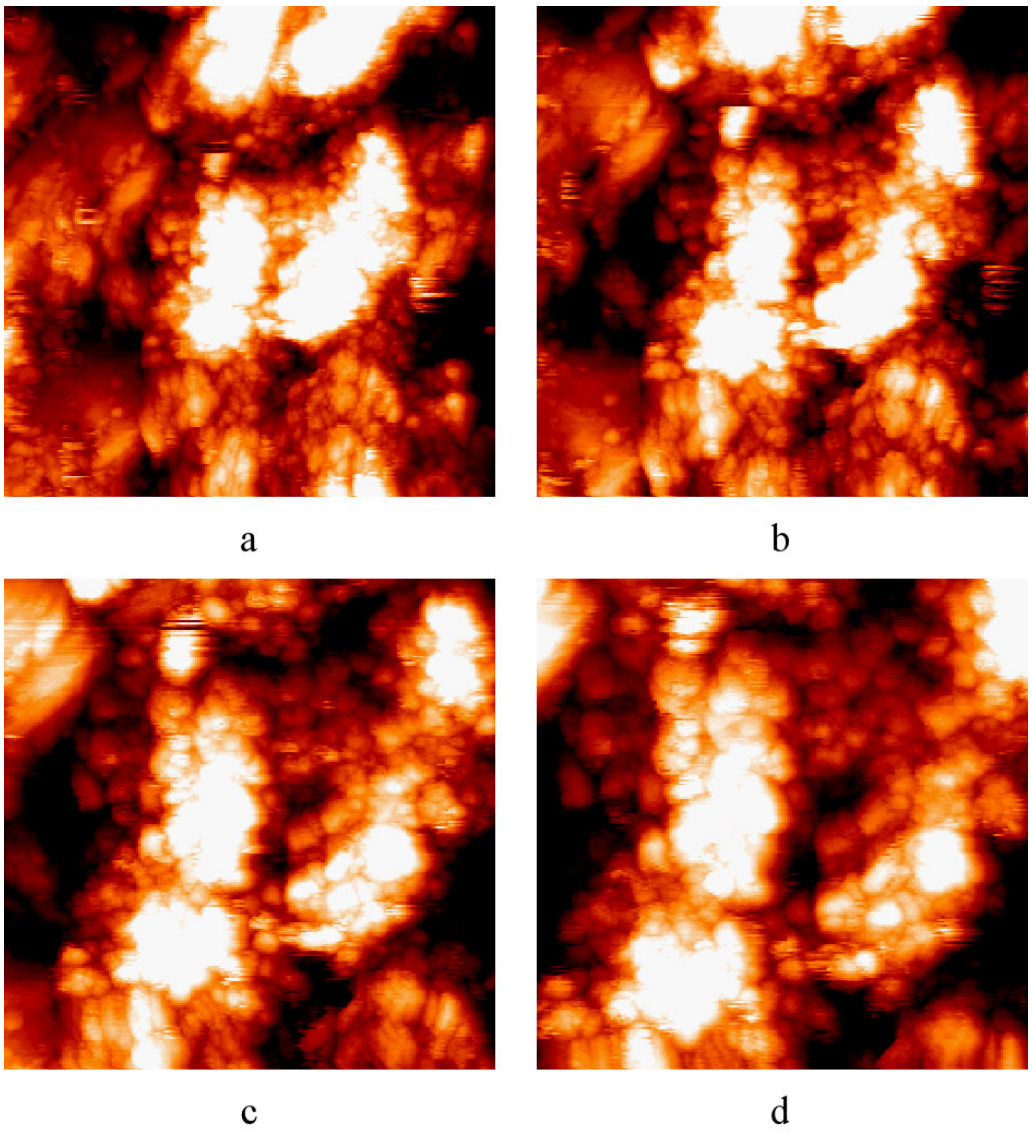

Figure 3.4 Diagnostic sample of Au on Si with tunneling conditions of 0.5 V and 1.0 nA with (a) scan size of 500 nm × 500 nm, (b) scan size of 400 nm × 400 nm, (c) scan size of 300 nm × 300 nm, and (d) scan size of 250 nm × 250 nm.

The tunneling conditions for these images vary slightly due to the increasing magnification of each image. At the scan sizes in Figure 3.4, we expected to see large features but not atomic resolution.

3.5.2 Graphite

HOPG was scanned next because of the smaller features contained on the surface. The images in Figure 3.5 show atomic resolution on graphite.

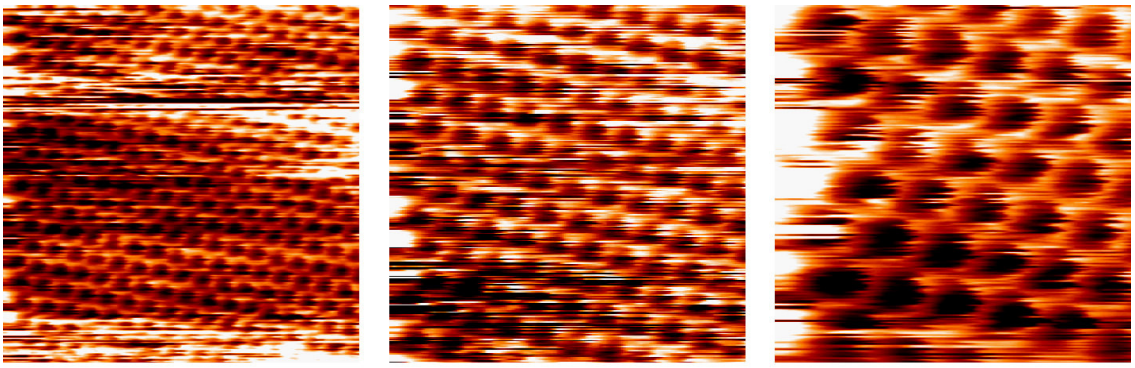

a b c

Figure 3.5 Diagnostic sample of graphite with tunneling conditions of 0.02 V, 7 nA with scan sizes of (a) 4 nm × 4 nm, (b) 2.5 nm × 2.5 nm, and (c) 1.5 nm × 1.5 nm.

3.5.3 Au(111)

The final diagnostic sample considered was gold on mica; the most difficult to obtain atomic resolution. The images in Figure 3.6 show atomic resolution of the Au(111) surface that occurs with gold on mica. There are four images in Figure 3.6, each with a progressively greater magnification of gold on mica. The differing tunneling conditions were only the scan size and the scan speed. As magnification of the surface increases, our view of the gold surface changes from the larger herringbone

reconstruction in Figure 3.6(a) to the single atom resolution in Figure 3.6(d) with each white feature representing a gold atom.

Once these images were acquired, it was known that the microscope was now ready to scan single molecules on the surface. Although there was a small amount of noise, this was deemed acceptable for scanning single molecules.

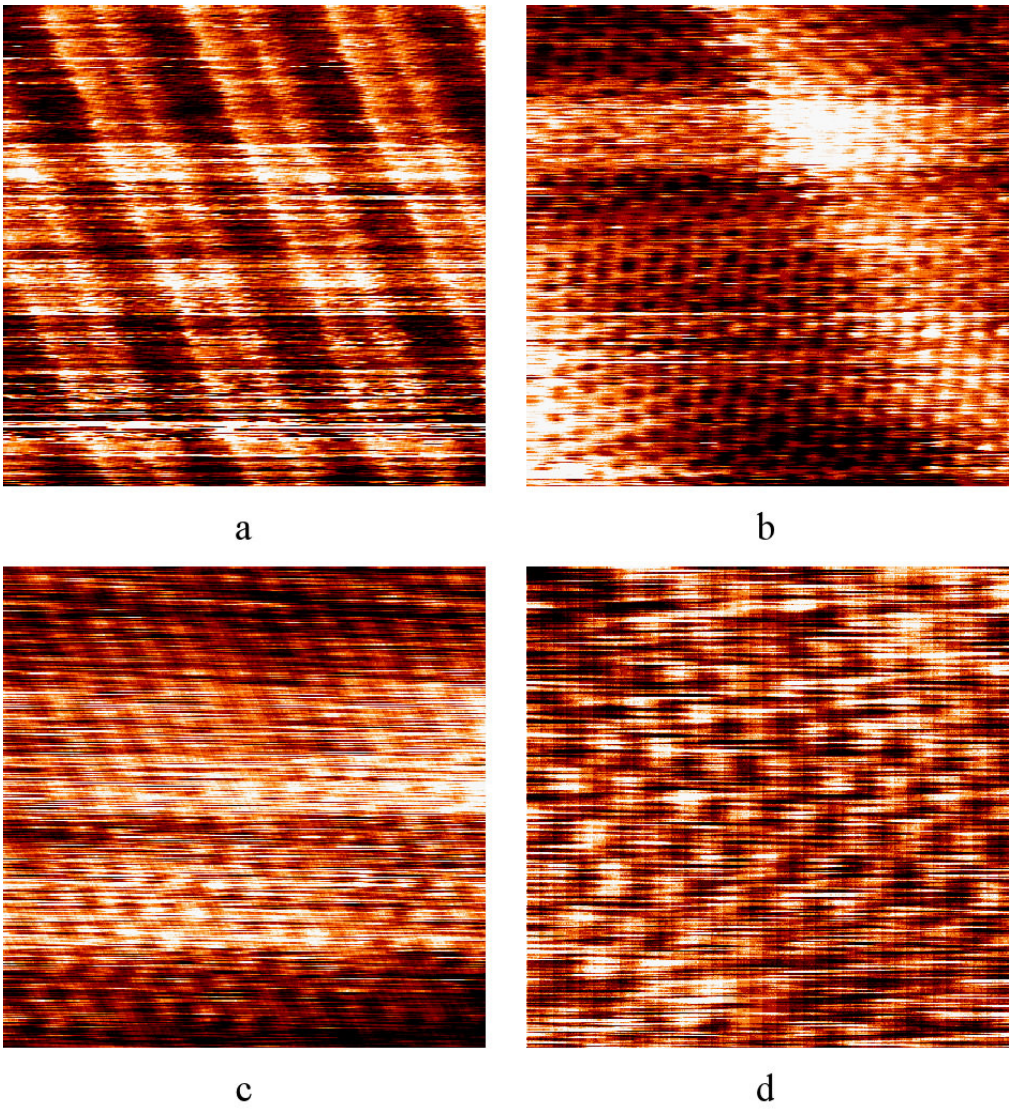

Figure 3.6 Diagnostic images of an Au(111) surface with tunneling conditions of 0.5 V, 1.5 nA, with scan sizes of (a) 25 nm × 25 nm, (b) 5 nm × 5 nm, (c) 3.5 nm × 3.5 nm, and (d) 2.5 nm × 2.5 nm

CHAPTER 4

RESULTS

4.1 Copper Phthalocyanine

The phthalocyanine studied in this thesis contains a copper atom as the center metal atom and has an octane chain attached to the outer carbon atoms. Figure 4.1 shows the structure of the phthalocyanine.

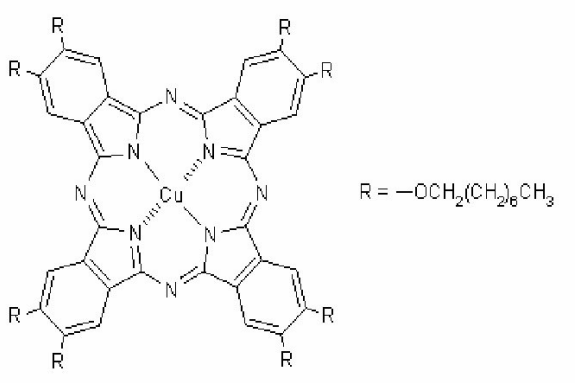

Figure 4.1 Figure of copper phthalocyanine

The molecule depicted in Figure 4.1 was readily available. The octane chains attached to the outer carbon atoms served as an advantage for the commencement of studies of single phthalocyanine molecules. These chains are rather long and may have stabilized the molecule on the surface.

Phthalocyanine was dip cast onto the surface for 30 seconds from a 2.75 μM methylene chloride solution. Once dry, the sample was transferred into the vacuum chamber. The approximate amount of time from dip casting to scanning was 30 minutes. The following experiments were done at 298 K.

4.2 Bias Voltage

The initial focus was the tunneling conditions that would best show the phthalocyanine on the surface with sub-molecular resolution.

4.2.1 Positive Bias

In Figure 4.2, the two parameters that were changed after each scan were the bias voltage and the scan area.

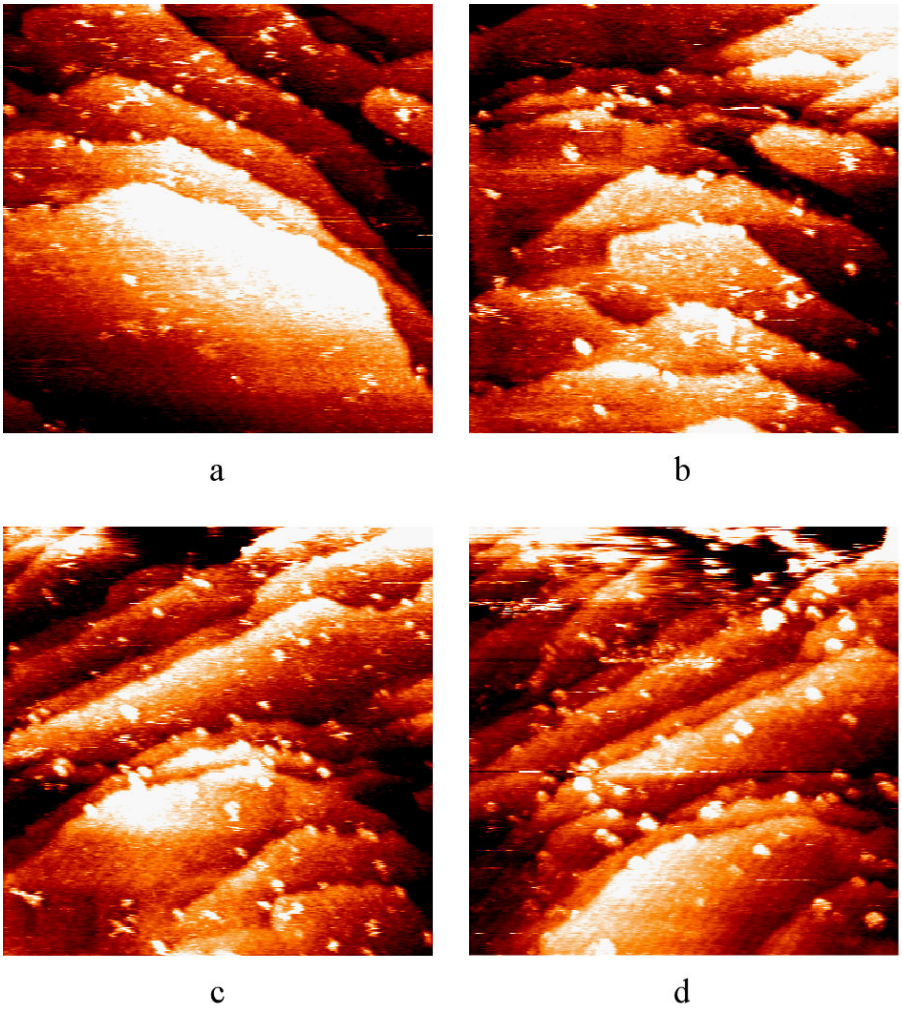

Figure 4.2 Images of copper phthalocyanines on a clean Au(111) surface with tunneling conditions of 0.025 nA, 125 nm × 125 nm and (a) 0.125 V, (b) 0.25 V, (c) 0.5 V, and (d) 1.0 V.

The white features in the Figure 4.2 images are the phthalocyanines molecules. The molecules are spread out over the surface, however, the majority are positioned near step edges. The fact that the majority are positioned near step edges demonstrate that the molecules may be more stabile when sitting at a step edge. The white features have an approximate size of 7 nm × 7 nm, which is larger than the measured size of this phthalocyanine, which is approximately 2.9 nm × 2.9 nm. After scanning the

gold surface, the microscope was calibrated, and therefore we know that the molecules imaged are larger than a single phthalocyanine.

4.2.2 Large Feature Size

There are possible explanations for the large size of the imaged molecules. There may be small groups of phthalocyanines clumping together. At these scan sizes if more than one phthalocyanines become associated with another, the groups of phthalocyanines appear as a single imaged feature on the surface. The molecules may be imaging larger because of the possible rotations that may occur with phthalocyanine molecules. If a portion of a molecule were rotating about a portion of itself, this would make the molecule appear larger than what it actually is.[1] A method of distinguishing between whether the white features are single phthalocyanines rotating, or alternatively are groups of phthalocyanines, is by observing the shape of each spot. If a feature is a single rotating molecule, the feature would be symmetrical. If the white features are groups of phthalocyanines, they could be different shapes and sizes.

Based on Figure 4.2, the white features are all different shapes and sizes, meaning that each feature is likely a group of phthalocyanines. The individual phthalocyanines in each group may also be rotating, creating diverse shapes and sizes, and making it difficult to determine the number of phthalocyanines affiliated with each group. It may be that phthalocyanines are grouping together for stability. The grouping of the molecules and positioning near a step edge may stabilize the

molecule enough to minimize translational motion, keeping the groups in the same general area.

These images also show that the phthalocyanines gravitate toward step edges. The step edges must stabilize the molecules and lower the translational motion of the phthalocyanines. There is some noise in these images. The ripples that appear between groups of phthalocyanines were a sort of periodic noise.

4.2.3 Reverse Bias

The images in Figure 4.2 were all taken with the same polarity of bias. In Figure 4.3, the bias polarity was reversed.

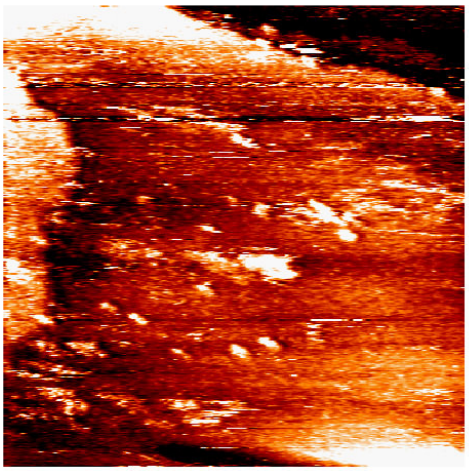

Figure 4.3 Copper phthalocyanines on a Au(111) surface with a reversed bias and tunneling conditions of -1.0 V, 0.05 nA, and 100 nm × 100 nm

Once the bias voltage polarity is reversed, the image changes. Large features on the surface can still be seen, such as the clusters of phthalocyanines in Figure 4.3. Detailed information would have been difficult to attain if large features on the surface look blurry at this scan size. As the images become smaller, the detail in the

images gradually becomes worse. Throughout the remainder of this thesis the discussion and images assume a positive bias polarity.

4.3 Magnification

Once it was determined the bias polarity should be positive, we began to magnify small clusters of molecules. Figure 4.4 is the first magnification of an area that contains small groups of phthalocyanines.

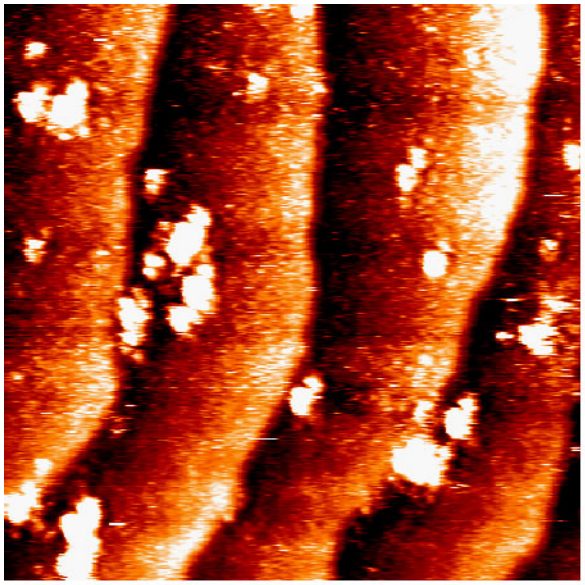

Figure 4.4 Copper phthalocyanines on a Au(111) surface with tunneling conditions of 1.0 V, 0.05 nA, and 83 nm × 83 nm

Figure 4.4 shows that the phthalocyanines are drawn to the step edges on the Au(111) surface. Since there are no distinct features within the molecules that can be discerned there are two possible explanations. The molecules may continue to be in motion or the tip may be blunt, or it may be a combination of the two. The sizes of the white features in Figure 4.4 vary in size and shape, indicating that there are groups of phthalocyanines. Also, feature sizes range from 2.5 nm to 10 nm, which

indicate that the features vary from a possible single phthalocyanine to a larger group of phthalocyanines.

4.4 Cluster Magnification

The magnification of the phthalocyanines was increased in Figure 4.5. Figure 4.5(a) and (b) are the same magnification, yet the phthalocyanine groups do not appear to be in the same place.

Figure 4.5(a) was taken first. In Figure 4.5(a) there appears six white features spread near the edge of the gold terrace. These six features are labeled: feature (i) appears to be separated into three areas along the terrace, with a size of 8.15 nm × 3 nm . Feature (ii) consists of two white clusters bridged together, with a size of 6.1 nm × 3 nm. Feature (iii) has a concentration of white at the center with halo of white coloring. Feature (iv) is a large white spot, with a size of 5 nm × 4.1 nm, that has some smearing protruding from the center. Feature (v) is the largest white spot with a protrusion stemming from the end and a size of 6.1 nm × 6.1 nm. Feature (vi) is two white spots that are close to the terrace and each spot is 3 nm × 3 nm . The phthalocyanines in Figure 4.5(a) are satisfactorily stabilized. There is not a doughnut shape present in any of the white features in the images, which would indicate a single rotating phthalocyanine molecule. Figure 4.5(b) was taken immediately after Figure 4.5(a), and show that the white features have moved.

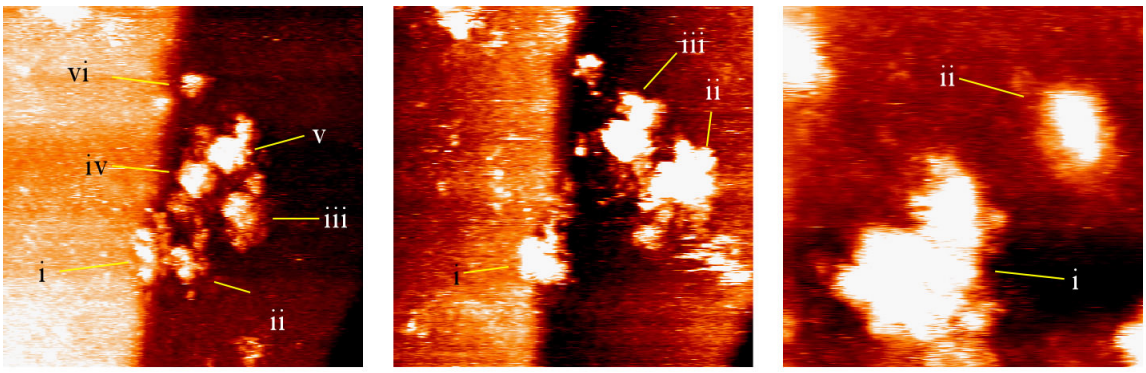

a b c

Figure 4.5 Copper phthalocyanines on a Au(111) surface with tunneling conditions for images (a) 1.0 V, 0.05 nA, and 42.8 nm × 42.8 nm, (b) 1.0 V, 0.05 nA, and 42.8 nm × 42.8 nm, and (c) 1.0 V, 0.05 nA, and 14 nm × 14 nm.

There are four features in Figure 4.5(b). Feature (i), 5 nm × 6.1 nm, is located along the terrace border. Feature (ii), 8.15 nm × 8.15 nm, is a large white spot with smearing of color. Feature (iii) has the same characteristics as (ii), with a size of 10 nm × 6.1 nm.

Figure 4.5(c) is a magnification of Figures 4.5(a) and (b), focusing on one of the large white features. In Figure 4.5(c) there are three features, one of which is only partially scanned. The large white feature does not have any particular shape, though it is much larger than the size of a single phthalocyanine. The large white feature is 5.2 nm across, 3.9 nm high with a peak height of 6.5 nm, which should be compared to a single phthalocyanine which has a size of 2.9 nm × 2.9 nm. The smaller feature labeled (ii) in Figure 4.5(c), has an oblong shape that can be attributed to several possible explanations that are subsequently discussed in this thesis. The size of the oblong white feature is 3.25 nm × 1.63 nm, and this corresponds to a surface feature that could possibly be a single phthalocyanine.

4.5 Single Cluster Magnification

The cluster labeled (i) in Figure 4.5(c) of phthalocyanines was studied in more depth to discern whether the number of phthalocyanines can be determined. The images in Figure 4.6 were taken to determine if individual phthalocyanines could be observed.

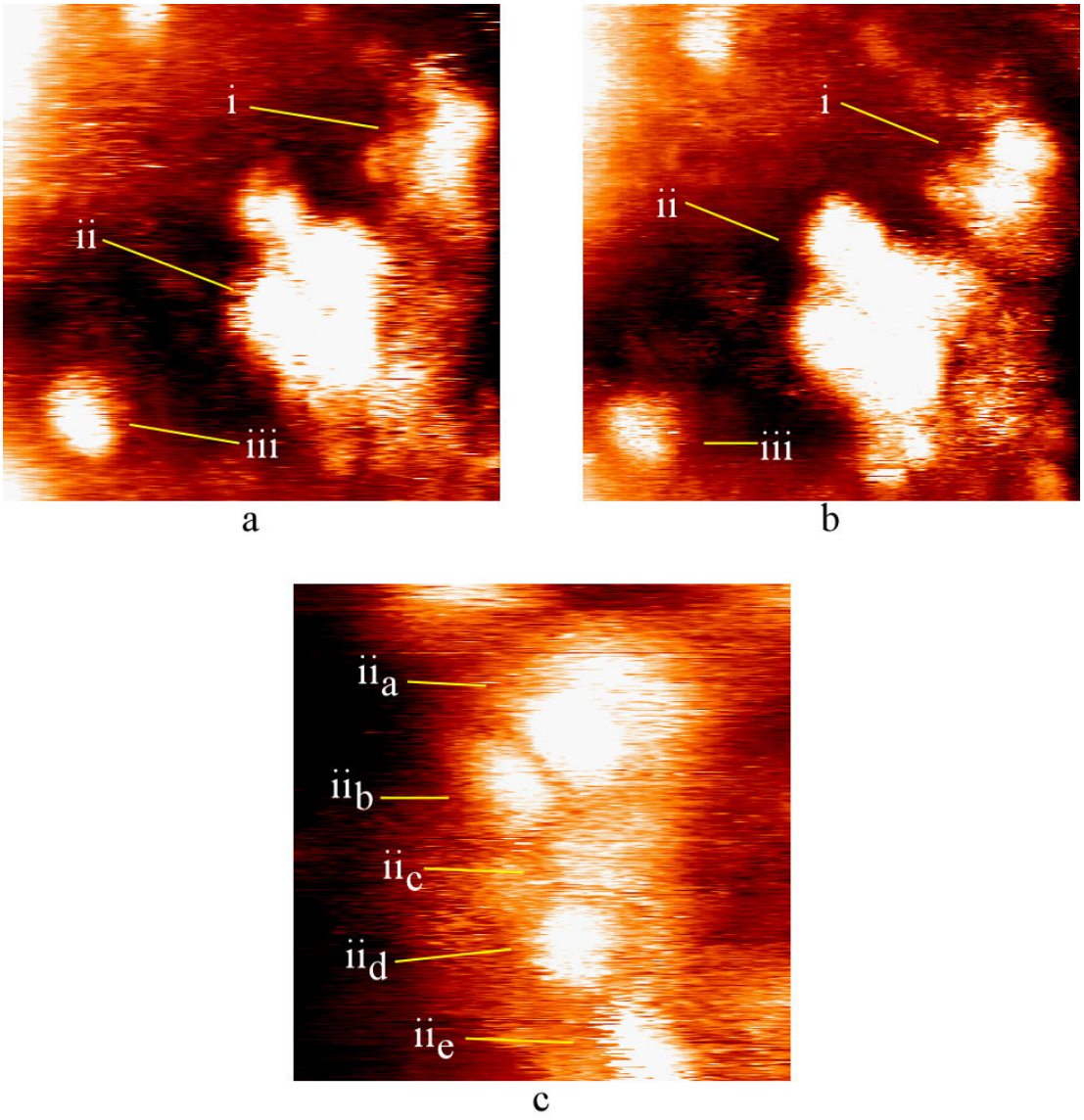

Figure 4.6 Close of copper phthalocyanines on a Au(111) surface with tunneling conditions of (a) 1.0 V, 0.0.5 nA, and 18 nm × 18 nm, (b) 1.0 V 0.05 nA, and 18 nm × 18 nm, and (c) 1.0 V, 0.05 nA, and 7.38 nm × 7.38 nm

The small white feature in Figure 4.6(a) labeled (iii) is approximately 2.8 nm × 1.7 nm, which is near the size of a phthalocyanine molecule. The large cluster labeled (ii) at the center of Figure 4.6(a) is 5.6 nm at the widest point and 7.9 nm at the longest point. The white cluster labeled (i) is 3.4 nm at the longest point and 2 nm at

the widest point. Both clusters labeled (i) and (ii) are larger than a single phthalocyanine would appear on the surface.

The clusters labeled (i)-(iii) in Figure 4.6(b) remained in roughly the same spot on the surface, but there are small differences between Figure 4.6(a) and (b). Cluster (i) has become sharper, revealing two round shapes within the cluster. The sizes of these two round shapes are 2.5 nm × 2.5 nm. Cluster (ii) appears to be the same size in Figure 4.6(b), however the resolution appears to have deteriorated slightly. There are no longer distinguishable groups in the larger white feature, and the size remains 5.6 nm at the widest point but now is 9 nm at the longest point. Cluster (iii) has become smaller in Figure 4.6(b), and has changed from 2.8 nm × 1.7 nm to 2.6 nm × 1.4 nm. There is a similarity shown in both Figures 4.6(a) and (b) for cluster (iii) in that there is a light halo surrounding cluster (iii). In Figure 4.6(b) the halo is larger and the white portion is smaller.

Figure 4.6(c) is a magnification of the large group of molecules labeled (ii) in Figures 4.6(a) and (b). The sizes of the white features shown in Figure 4.6(c) are listed in Table 4.1. These measurements were taken omitting the light halo around all the white features.

TABLE 4.1

CLUSTER SIZES OF THOSE FOUND IN FIGURE 4.6(c)

Cluster	Widest Point	Longest Point
ii_a	5.4 nm	5.4 nm
ii_b	1.8 nm	3.6 nm
ii_c	3.6 nm	2.4 nm
ii_d	2.4 nm	2.4 nm
ii_e	2.4 nm	N/A

The larger feature labeled (ii_a) in Figure 4.6(c) is of a size that indicates it may consist of two phthalocyanines that are located next to each other. White feature (ii_b) is of a size consistent with a single phthalocyanine. White feature (ii_c) appears to be shading that is present between groups (ii_a) and (ii_d). The size of (ii_d) corresponds to a single phthalocyanine molecule. Although the measurements of features (ii_b) and (ii_d) are not equivalent, there are explanations as to why they still may represent a single phthalocyanine. For instance, the molecular movement of each particular phthalocyanine can alter the size measurement. The final portion in Figure 4.6(c) is (ii_e), though the size of this feature cannot be measured because part of that group is outside the scan window. From what is seen; feature (ii_e) represents a possible single phthalocyanine that is in motion. The width of the feature (ii_e) is consistent with the width of a single phthalocyanine. The length of this feature, however, shows that the molecule is likely to be in motion on the surface. Feature (ii_e) is being stretched in one particular direction. Once the cluster is magnified, the movement of phthalocyanines within that cluster can be observed.

4.6 References

1. Hersam, M.C., N.P. Guisinger, and J.W. Lyding, *Isolating, imaging, and electrically characterizing individual organic molecules on the Si(100) surface with the scanning tunneling microscope.* Journal of Vacuum Science & Technology a-Vacuum Surfaces and Films, 2000. **18**(4): p. 1349-1353.

CHAPTER 5

DISCUSSION

There are several explanations for the behavior of the molecules observed in Figures 4.4-4.6. When the white features appear larger than a single phthalocyanine, there is either some molecular motion that it is making the phthalocyanine appear larger, or there are more than one phthalocyanine associated with that white feature.

5.1 Molecular Motion

Molecular motion may have been facilitated through different sources. Those sources may have been either thermal motion or tip induced movement. These scans were taken at approximately 298K, with a coverage less than a full monolayer The binding energy of phthalocyanines to a gold surface may be low enough for thermal effects to take over and cause the molecules to move on the surface.

The motion could have been tip induced.[1-8] As electrons are tunneling from the tip into the surface, it is possible for surface molecules to interact with the tip and be pulled or pushed along the surface. This would indicate at this particular temperature, the binding energy of phthalocyanines to a gold surface is low enough that a small interaction may move the molecules on the surface.

Rotational motion can also affect imaging of single phthalocyanines. A portion of the phthalocyanine may be bound tighter to the gold surface and acting as

an axis of rotation.[9] This axis of rotation may have arisen from a small defect in the surface or from the manner in which a small group of phthalocyanines bunched together. One characteristic of a molecule rotating around a single nitrogen atom is the symmetry of the white feature in the image.

White features can also look larger than single phthalocyanines because there may be more than one phthalocyanine associated with that feature. Phthalocyanines have shown stability when they are laid down in a full monolayer coverage. The molecules find stability when interacting with each other. If two or three phthalocyanines are interacting with each other in close proximity, they may become more stable. If more than one phthalocyanine are moving in unison, the white spot may appear quite large compared to a stationary single phthalocyanine. In Figures 4.4-4.6 there is no molecular resolution, making it difficult to discern whether there are more than one phthalocyanines associated with each white feature.

5.2 Figure 4.5 Discussion

Figure 4.5 contains two consecutive images that display possible molecular movement. This movement appears to have created larger groups of phthalocyanines. The halo that appears around the large groups in Figure 4.5 may be more phthalocyanines. The bright white features may be phthalocyanines stacked upon other phthalocyanines, making the features appear taller during scanning. If the halo consists of more phthalocyanines, it would explain why there are fewer white features in Figure 4.5(b), and why those features are larger than the white features in Figure 4.5(a). In short, the size of the clusters may be attributed to the number of

phthalocyanines affiliated with each cluster, the rotational motion of each phthalocyanine within the cluster, and the translational motion of the entire group.

Figure 4.5(c) displays a large group of phthalocyanines as well as a possible single phthalocyanines. The measurements of the possible single phthalocyanine are asymmetrical, which may stem from translational motion of the molecule. The molecule may have been moving in a way that would cause it to become elongated in one direction, and become shorter in another direction. The resolution of the image is not clear enough to distinguish the number of different molecules comprising the group, and this is due to molecular motion.

5.3 Figure 4.6 Discussion

The images in Figure 4.6 demonstrate some of the same characteristics as those in Figure 4.5. Although there is not sub-molecular resolution in Figure 4.6, there are observations that help explain the behavior of the clusters in these images.

The comparative quality of the resolution between Figure 4.6(a) and (b) is improved in some instances, and becomes worse in others. In particular, the group labeled (i), in Figure 4.6(b) separates into what appears to be two distinct entities. These features are symmetrical, and the same size, which indicates that there are two molecules located next to each other. The resolution of the larger feature (ii) has deteriorated slightly, and the number of molecules that compromise (ii) cannot be discerned from Figure 4.6(b). Movement of feature (ii) lowered the resolution making it difficult to determine the number of phthalocyanines in that particular group. The group labeled (iii) becomes slightly smaller in Figure 4.6(b). This change

can be attributed to one or several of the following: a change in tip structure, molecular movement induced by the tip, or thermal energy moving the phthalocyanine.

Feature (ii_c) in Figure 4.6(c) is of particular interest. Feature (ii_c) is shadowed throughout the image indicating possible motion within that group of phthalocyanines. Although all the phthalocyanines are most likely in motion, feature (ii_c) seems to be bouncing back and forth between features (ii_a) and (ii_e). A possible explanation for this bouncing is that both features (ii_a) and (ii_e) are bound more strongly to the surface, creating a situation in which the force of each collision from (ii_c) does not induce motion. Feature (ii_c) could be located on a portion of the gold surface that has a small imperfection underneath the phthalocyanine, not allowing the molecule to sit and obtain an energetically favorable position. Unfortunately, this trapped position does not stabilize the molecule enough to reach sub-molecular resolution. There is no sub-molecular resolution throughout Figure 4.6(c), which may be due to tip changes, induced molecular motion, or thermally induced molecular motion.

5.4 Conclusion

Figures 4.4-4.6 do not show sub-molecular resolution for single phthalocyanines. However, we have demonstrated that phthalocyanines may be placed on a surface at a low coverage and then studied using STM. Dip-casting is a viable option for placing phthalocyanines on a gold surface. At a low enough concentration the surface coverage of phthalocyanines is sparse enough to study individual molecules.

Scanning at 298 K is reasonable, but it is possible that at this temperature there exists excess thermal energy associated with the surface molecules that prevents them from remaining stationary. Gold is a viable surface to study single phthalocyanines.

There are certain aspects of this project that can be altered to further study single phthalocyanines. The sample temperature can be cooled to liquid nitrogen temperatures. At such a reduced temperature, there may be enough thermal energy removed from the system so that the surface molecules will remain stationary. Although, if at this temperature the molecules are still not stationary, it is possible to lower the temperature even further and see if at liquid helium temperatures the molecules will become stationary. The surface may be changed to graphite, or another metal, or a self assembled monolayer. If the surface provides sufficient stabilization the molecules will remain stationary. This would increase the chance of finding a single phthalocyanine that has no molecular motion. The phthalocyanine studied can be changed as well, perhaps elongating the alkane chains attached to the pi-structure, these longer chains may stabilize the molecule, keeping it stationary. Changing these parameters may help understand the underlying physical and electronic properties of phthalocyanines. Once these principles are understood, perhaps they can be utilized to construct a working QCA system in which simple calculations can be done.

5.5 References

1. Moresco, F., *Manipulation of large molecules by low-temperature STM: model systems for molecular electronics.* Physics Reports-Review Section of Physics Letters, 2004. **399**(4): p. 175-225.

2. Kurnosikov, O., J.T. Kohlhepp, and W.J.W. de Jonge, *STM-tip induced displacement of Co atoms embedded in a Cu(001) surface.* Surface Science, 2004. **566**: p. 175-180.

3. Dulot, F., J. Eugene, B. Kierren, and D. Malterre, *STM-TIP induced surface diffusion of copper on copper (100).* Applied Surface Science, 2000. **162**: p. 86-93.

4. Kurpick, U. and T.S. Rahman, *Tip induced motion of adatoms on metal surfaces.* Physical Review Letters, 1999. **83**(14): p. 2765-2768.

5. Bohringer, M., W.D. Schneider, and R. Berndt, *Scanning tunneling microscope-induced molecular motion and its effect on the image formation.* Surface Science, 1998. **408**(1-3): p. 72-85.

6. Moller, R., R. Coenen, A. Esslinger, and B. Koslowski, *The Topography of Isolated Molecules of Copper-Phthalocyanine Adsorbed on Gaas(110).* Journal of Vacuum Science & Technology a-Vacuum Surfaces and Films, 1990. **8**(1): p. 659-660.

7. Chiang, S., *Scanning tunneling microscopy imaging of small adsorbed molecules on metal surfaces in an ultrahigh vacuum environment.* Chemical Reviews, 1997. **97**(4): p. 1083-1096.

8. Lorente, N., R. Rurali, and H. Tang, *Single-molecule manipulation and chemistry with the STM.* Journal of Physics-Condensed Matter, 2005. **17**(13): p. S1049-S1074.

9. Hersam, M.C., N.P. Guisinger, and J.W. Lyding, *Isolating, imaging, and electrically characterizing individual organic molecules on the Si(100) surface with the scanning tunneling microscope.* Journal of Vacuum Science & Technology a-Vacuum Surfaces and Films, 2000. **18**(4): p. 1349-1353.

BIBLIOGRAPHY

1. Bao, Z.A., A.J. Lovinger, and J. Brown, *New air-stable n-channel organic thin film transistors.* Journal of the American Chemical Society, 1998. **120**(1): p. 207-208.

2. Barlow, D.E., L. Scudiero, and K.W. Hipps, *Scanning tunneling microscopy study of the structure and orbital-mediated tunneling spectra of cobalt(II) phthalocyanine and cobalt(II) tetraphenylporphyrin on Au(111): Mixed composition films.* Langmuir, 2004. **20**(11): p. 4413-4421.

3. Bohringer, M., R. Berndt, and W.D. Schneider, *Transition from three-dimensional to two-dimensional faceting of Ag(110) induced by Cu-phthalocyanine.* Physical Review B, 1997. **55**(3): p. 1384-1387.

4. Bohringer, M., W.D. Schneider, and R. Berndt, *Scanning tunneling microscope-induced molecular motion and its effect on the image formation.* Surface Science, 1998. **408**(1-3): p. 72-85.

5. Carroll, R.L. and C.B. Gorman, *The genesis of molecular electronics.* Angewandte Chemie-International Edition, 2002. **41**(23): p. 4379-4400.

6. Chiang, S., *Scanning tunneling microscopy imaging of small adsorbed molecules on metal surfaces in an ultrahigh vacuum environment.* Chemical Reviews, 1997. **97**(4): p. 1083-1096.

7. Chizhov, I., G. Scoles, and A. Kahn, *The influence of steps on the orientation of copper phthalocyanine monolayers on Au(111).* Langmuir, 2000. **16**(9): p. 4358-4361.

8. Collins, R.A. and K.A. Mohammed, *Gas Sensitivity of Some Metal Phthalocyanines.* Journal of Physics D-Applied Physics, 1988. **21**(1): p. 154-161.

9. Crone, B., A. Dodabalapur, Y.Y. Lin, R.W. Filas, Z. Bao, A. LaDuca, R. Sarpeshkar, H.E. Katz, and W. Li, *Large-scale complementary integrated circuits based on organic transistors.* Nature, 2000. **403**(6769): p. 521-523.

10. Dulot, F., J. Eugene, B. Kierren, and D. Malterre, *STM-TIP induced surface diffusion of copper on copper (100).* Applied Surface Science, 2000. **162**: p. 86-93.

11. Garnier, F., Thin-film transistors based on organic conjugated semiconductors. Chemical Physics, 1998. 227(1-2): p. 253-262.

12. Gimzewski, J.K., E. Stoll, and R.R. Schlittler, *Scanning Tunneling Microscopy of Individual Molecules of Copper Phthalocyanine Adsorbed on Polycrystalline Silver Surfaces.* Surface Science, 1987. **181**(1-2): p. 267-277.

13. Grand, J.Y., T. Kunstmann, D. Hoffmann, A. Haas, M. Dietsche, J. Seifritz, and R. Moller, *Epitaxial growth of copper phthalocyanine monolayers on Ag(111).* Surface Science, 1996. **366**(3): p. 403-414.

14. Hersam, M.C., N.P. Guisinger, and J.W. Lyding, *Isolating, imaging, and electrically characterizing individual organic molecules on the Si(100) surface with the scanning tunneling microscope.* Journal of Vacuum Science & Technology a-Vacuum Surfaces and Films, 2000. **18**(4): p. 1349-1353.

15. Hiesgen, R., M. Rabisch, H. Bottcher, and D. Meissner, *STM investigation of the growth structure of Cu-phthalocyanine films with submolecular resolution.* Solar Energy Materials and Solar Cells, 2000. **61**(1): p. 73-85.

16. Hipps, K.W., X. Lu, X.D. Wang, and U. Mazur, *Metal d-orbital occupation-dependent images in the scanning: Tunneling microscopy of metal phthalocyanines.* Journal of Physical Chemistry, 1996. **100**(27): p. 11207-11210.

17. Inabe, T. and H. Tajima, *Phthalocyanines - Versatile components of molecular conductors.* Chemical Reviews, 2004. **104**(11): p. 5503-5533.

18. James, D.K. and J.M. Tour, *Electrical measurements in molecular electronics.* Chemistry of Materials, 2004. **16**(23): p. 4423-4435.

19. Jung, T.A., R.R. Schlittler, J.K. Gimzewski, H. Tang, and C. Joachim, *Controlled room-temperature positioning of individual molecules: Molecular flexure and motion.* Science, 1996. **271**(5246): p. 181-184.

20. Kanai, M., T. Kawai, K. Motai, X.D. Wang, T. Hashizume, and T. Sakura, *Scanning-Tunneling-Microscopy Observation of Copper-Phthalocyanine Molecules on Si(100) and Si(111) Surfaces.* Surface Science, 1995. **329**(3): p. L619-L623.

21. Kurnosikov, O., J.T. Kohlhepp, and W.J.W. de Jonge, *STM-tip induced displacement of Co atoms embedded in a Cu(001) surface.* Surface Science, 2004. **566**: p. 175-180.

22. Kurpick, U. and T.S. Rahman, *Tip induced motion of adatoms on metal surfaces.* Physical Review Letters, 1999. **83**(14): p. 2765-2768.

23. Lei, S.B., C. Wang, S.X. Yin, and C.L. Bai, *Single molecular arrays of phthalocyanine assembled with nanometer sized alkane templates.* Journal of Physical Chemistry B, 2001. **105**(49): p. 12272-12277.

24. Lent, C.S. and P.D. Tougaw, *Lines of Interacting Quantum-Dot Cells - a Binary Wire.* Journal of Applied Physics, 1993. **74**(10): p. 6227-6233.

25. Lent, C.S., P.D. Tougaw, and W. Porod, *Bistable Saturation in Coupled Quantum Dots for Quantum Cellular Automata.* Applied Physics Letters, 1993. **62**(7): p. 714-716.

26. Lent, C.S. and P.D. Tougaw, *Bistable Saturation Due to Single-Electron Charging in Rings of Tunnel-Junctions.* Journal of Applied Physics, 1994. **75**(8): p. 4077-4080.

27. Lent, C.S., B. Isaksen, and M. Lieberman, *Molecular quantum-dot cellular automata.* Journal of the American Chemical Society, 2003. **125**(4): p. 1056-1063.

28. Lippel, P.H., R.J. Wilson, M.D. Miller, C. Woll, and S. Chiang, *High-Resolution Imaging of Copper-Phthalocyanine by Scanning-Tunneling Microscopy.* Physical Review Letters, 1989. **62**(2): p. 171-174.

29. Lorente, N., R. Rurali, and H. Tang, *Single-molecule manipulation and chemistry with the STM.* Journal of Physics-Condensed Matter, 2005. **17**(13): p. S1049-S1074.

30. Ludwig, C., R. Strohmaier, J. Petersen, B. Gompf, and W. Eisenmenger, *Epitaxy and Scanning-Tunneling-Microscopy Image-Contrast of Copper Phthalocyanine on Graphite and Mos2.* Journal of Vacuum Science & Technology B, 1994. **12**(3): p. 1963-1966.

31. Madru, R., G. Guillaud, M. Alsadoun, M. Maitrot, J.J. Andre, J. Simon, and R. Even, *A Well-Behaved Field-Effect Transistor Based on an Intrinsic Molecular Semiconductor.* Chemical Physics Letters, 1988. **145**(4): p. 343-346.

32. Maitrot, M., G. Guillaud, B. Boudjema, J.J. Andre, H. Strzelecka, J. Simon, and R. Even, *Lutetium Bisphthalocyanine - the 1st Molecular Semiconductor - Conduction Properties of Thin-Films of P-Doped and N-Doped Materials.* Chemical Physics Letters, 1987. **133**(1): p. 59-62.

33. Manimaran, M., G.L. Snider, C.S. Lent, V. Sarveswaran, M. Lieberman, Z.H. Li, and T.P. Fehlner, *Scanning tunneling microscopy and spectroscopy investigations of QCA molecules.* Ultramicroscopy, 2003. **97**(1-4): p. 55-63.

34. Mantooth, B.A. and P.S. Weiss, *Fabrication, assembly, and characterization of molecular electronic components.* Proceedings of the Ieee, 2003. **91**(11): p. 1785-1802.

35. Moller, R., R. Coenen, A. Esslinger, and B. Koslowski, *The Topography of Isolated Molecules of Copper-Phthalocyanine Adsorbed on Gaas(110).* Journal of Vacuum Science & Technology a-Vacuum Surfaces and Films, 1990. **8**(1): p. 659-660.

36. Moresco, F., *Manipulation of large molecules by low-temperature STM: model systems for molecular electronics.* Physics Reports-Review Section of Physics Letters, 2004. **399**(4): p. 175-225.

37. Orlov, A.O., I. Amlani, R.K. Kummamuru, R. Ramasubramaniam, G. Toth, C.S. Lent, G.H. Bernstein, and G.L. Snider, *Experimental demonstration of clocked single-electron switching in quantum-dot cellular automata.* Applied Physics Letters, 2000. **77**(2): p. 295-297.

38. Orlov, A.O., R. Kummamuru, R. Ramasubramaniam, C.S. Lent, G.H. Bernstein, and G.L. Snider, *Clocked quantum-dot cellular automata shift register.* Surface Science, 2003. **532**: p. 1193-1198.

39. Packan, P.A., *Perspectives: Device physics - Pushing the limits.* Science, 1999. **285**(5436): p. 2079-+.

40. Qiu, X.H., C. Wang, S.X. Yin, Q.D. Zeng, B. Xu, and C.L. Bai, *Self-assembly and immobilization of metallophthalocyanines by alkyl substituents observed with scanning tunneling microscopy.* Journal of Physical Chemistry B, 2000. **104**(15): p. 3570-3574.

41. Sanders, G.D., K.W. Kim, and W.C. Holton, *Optically driven quantum-dot quantum computer.* Physical Review A, 1999. **60**(5): p. 4146-4149.

42. Service, R.F., *Can chip devices keep shrinking?* Science, 1996. **274**(5294): p. 1834-1836.

43. Snider, G.L., A.O. Orlov, I. Amlani, X. Zuo, G.H. Bernstein, C.S. Lent, J.L. Merz, and W. Porod, *Quantum-dot cellular automata: Review and recent experiments (invited).* Journal of Applied Physics, 1999. **85**(8): p. 4283-4285.

44. Stohr, M., T. Wagner, M. Gabriel, B. Weyers, and R. Moller, *Binary molecular layers of C-60 and copper phthalocyanine on Au(111): Self-*

organized nanostructuring. Advanced Functional Materials, 2001. **11**(3): p. 175-178.

45. Toth, G. and C.S. Lent, *Quasiadiabatic switching for metal-island quantum-dot cellular automata.* Journal of Applied Physics, 1999. **85**(5): p. 2977-2984.

46. Tougaw, P.D. and C.S. Lent, *Logical Devices Implemented Using Quantum Cellular-Automata.* Journal of Applied Physics, 1994. **75**(3): p. 1818-1825.

47. Tour, J.M., *Molecular electronics. Synthesis and testing of components.* Accounts of Chemical Research, 2000. **33**(11): p. 791-804.

48. Walzer, K. and M. Hietschold, *STM and STS investigation of ultrathin tin phthalocyanine layers adsorbed on HOPG(0001) and Au(111).* Surface Science, 2001. **471**(1-3): p. 1-10.

49. Watson, M.D., F. Jackel, N. Severin, J.P. Rabe, and K. Mullen, *A hexa-peri-hexabenzocoronene cyclophane: An addition to the toolbox for molecular electronics.* Journal of the American Chemical Society, 2004. **126**(5): p. 1402-1407.